A Novel Floating-Gate Biosensing Device with Controlled Charge-Modulation

Chengwu Tao*, Baozhen Chen, Sumarlin William, Santosh Pandey
Department of Electrical and Computer Engineering,
Iowa State University,
Ames, IA, USA.
ctao@iastate.edu, pandey@iastate.edu

***Abstract* — A novel charge-modulated biosensing device is proposed. The basic architecture of an extended floating-gate field-effect transistor (FET) is modified for VLSI applications. The floating-gate is umbrella-shaped (UGFET), maximizing the charge sensing area in a much reduced device area. Compared to previous extended floating-gate structures, the UGFET shows improved scalability and sensitivity. Extensive device simulations validate the UGFET model. The design is fabricated in a standard CMOS process and characterized with electrolytes and charged solutions. Transconductance measurements confirm its high sensitivity and workability.**

I. Introduction

In recent years, solid-state biosensors are replacing chemical techniques that are often too cumbersome, time-consuming, and expensive [1-4]. There is a growing interest for CMOS-compatible, silicon sensors with direct electronic read-out [2]. In the past, a number of such devices have been reported but most of them require special post-processing steps not available in a standard CMOS foundry [1-3].

Few years ago, a charge-sensing concept based on extended floating-gate Field Effect Transistor (FET) was proposed [5, 6]. This **C**harge-**M**odulated **FET** (CMFET) has a floating-gate that is capacitively coupled to a sensing area on one side and to a control-gate on the other side (Fig. 1). Current induced in the transistor is dependent on the control voltage and charges on the sensing area. Any charge fluctuations directly affect the IV characteristics of the FET. There is no reference electrode needed and the fabrication can be carried out in a standard CMOS process [5].

Previous CMFET devices have been relatively large (typically 100x100μm) by the virtue of their design [5-7]. This limits their applications in VLSI circuits. In this work, we present a novel **FET** with an **U**mbrella-shaped Floating-**G**ate (UGFET). The UGFET architecture is still an extended floating-gate design but with an efficient floating-gate topology (Fig. 2). This drastically reduces the device area while preserving its charge-sensing attributes.

II. Methodology

An extended floating-gate CMFET is shown in Fig. 1 where a floating-gate is capacitively coupled to a sensing area (SA) and a control gate [5-7]. Our proposed extended floating-gate UGFET is illustrated in Fig. 2 with the various capacitances in play. Here, the floating-gate covers the entire

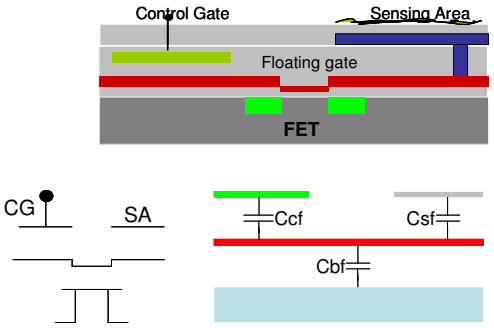

Fig. 1: (Top) Cross-section of a typical floating-gate biosensor (CMFET), and (Bottom) its symbolic representation with a capacitance model [5].

device to maximize the sensing area and minimize the lateral dimensions (compared to Fig. 1). In terms of the model parameters, floating-gate voltage V_{CG} can be written as [5]:

$$V_{FG} = \frac{C_{CF}}{C_{CF} + C_{FB} + C_{SF}} V_{CG} + \frac{Q_0 + Q_S}{C_{CF} + C_{FB} + C_{SF}} \qquad (1)$$

where V_{CG} denotes the control-gate voltage, Q_0 is the total charge trapped inside the floating gate, Q_S is the charge on the sensing area (SA in Fig.1) of the floating-gate. The capacitance between the floating-gate and control-gate is C_{SF} while the capacitance between the floating-gate and the substrate bulk is C_{SF}. Also, a capacitance C_{SF} results due to a spacer or passivation layer separating the floating-gate SA region from the actual biological sample.

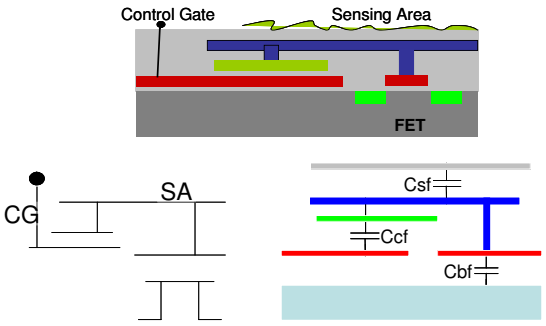

Fig. 2: (Top) Cross-section of the proposed floating-gate (UGFET) biosensor with a much efficient topology and reduced size, and (Bottom) its symbolic representation with a capacitance model.

978-1-4244-1813-8/08/$25.00 © 2008 IEEE

Authorized licensed use limited to: Iowa State University. Downloaded on May 16,2022 at 19:17:35 UTC from IEEE Xplore. Restrictions apply.

Since the floating-gate is completely isolated, its total charge must remain a constant. This charge conservation principle was used earlier to arrive at Eq. 1. We can rewrite Eq.1 as:

$$V_{FG} = \alpha V_{CG} + \frac{Q_0 + Q_S}{\beta} \quad (2)$$

where

$$\alpha = \frac{C_{CF}}{C_{CF} + C_{FB} + C_{SF}} \text{ and } \beta = \frac{C_{CF}}{\alpha} \quad (3)$$

It can be easily demonstrated that the UGFET's effective threshold voltage depends on the amount and nature of surface charges over the sensing area. Positive Q_S causes a negative shift in the effective threshold voltage, while negative Q_S gives a positive shift in the threshold voltage (for n-channel FETs) [6].

For simulation purposes, the UGFET biosensing device is designed using Scalable CMOS (SCMOS) design rules available through Cadence. The sensing area for the structure simulated is roughly 14.4µm×28.4 µm. A three-dimensional (3D) UGFET device model is constructed using Synopsys® Sentaurus Structure Device Editor. This device simulator is very user-friendly and helps create a realistic device structure according to the criteria later used for fabrication. The simulation process is beneficial in visualizing the redistribution of potentials and fields with charge fluctuations over the sensing area.

We show a snapshot of the UGFET structure built using the device simulator (Fig. 3). The semiconductor parameters are defined according to the MOSIS AMI 1.5µm technology. Using a 3D device model, α and β (defined in Eq. 3) are calculated taking into account all parasitics such as fringe capacitance and overlap capacitance. From the calculation, α_{3D} is estimated to be around 0.68 and β_{3D} is around 63.6fF. These values were approximately 9-12% greater than those obtained using a 1D model. In principle, as the device structure shrinks in dimensions, the 3D model gives a better representation of the device physics compared to a 1D model.

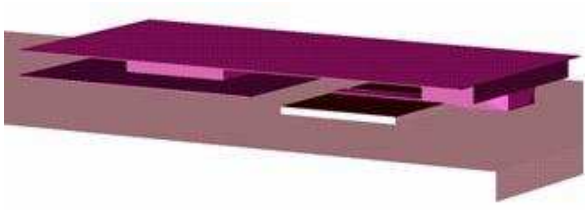

Fig. 3: Three-dimensional cross-section of our floating-gate device (UGFET) built with the Synopsis Sentaurus device simulator.

Among the several simulation results recorded, we show two key results. In Fig. 4, the control-gate voltage is swept from 0V to 10V. Two cases are plotted where the charge densities are 4×10^{10} electrons per square cm. and 8×10^{10} electrons per square cm. The spacer thickness separating the floating gate from external charges is 200nm. There exists a linear relationship between the floating-gate voltage and control-gate voltage (according to Eq. 1-3).

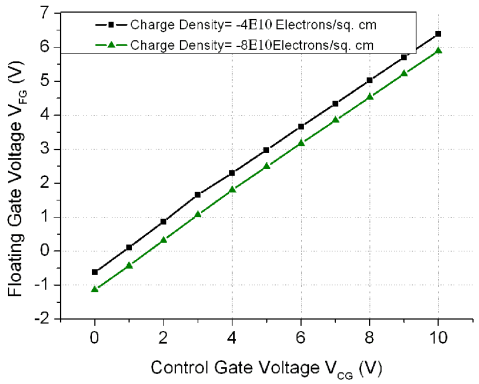

Fig. 4: Floating-gate voltage is linearly dependent on the control-gate voltage for the UGFET device as observed from the device simulations. The two plots are from two values of charge densities on the sensing area.

In Fig. 5, we show the dependence of floating-gate voltage on the charge density. The spacer thickness is chosen as 30nm. Three cases are plotted for three different control-gate voltages: 2V, 4V and 6V. Again, we see a linear relationship between the floating-gate voltage and charge density to be sensed. This follows from Eq. 1-3. Furthermore, the floating-gate voltage also depends on the spacer thickness. A thicker spacer induces less potential on the floating-gate but this dependence is quite insignificant.

During an experiment, the amount of charge (e.g. from single-strand oligonucleotides) immobilized on the sensing area can be easily modified and this, in turn, will modulate the UGFET's threshold voltage [5]. The shift in threshold voltage is usually determined by measuring the drain current at a constant control-gate voltage or by measuring the control-gate voltage at a constant drain current. The topic is further discussed in the next section. The electronics instrumentation can also be programmed to repeat the device measurements over a period of time. This would help detect and monitor any subtle charge fluctuations due to some chemical reactions over the sensing area (e.g. DNA hybridization or neuronal communication) [8].

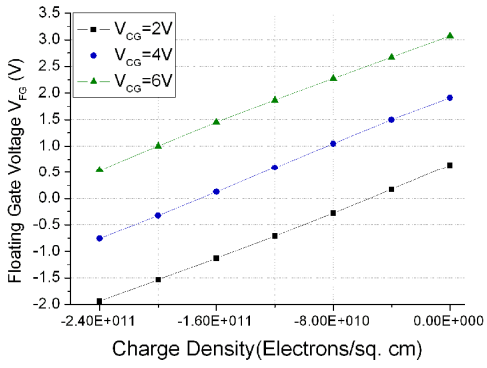

Fig. 5: Simulation results show the floating-gate voltage is linearly dependent on the charge density over the sensing area of UGFET device. The three plots are related to three values of the control-gate voltage.

Authorized licensed use limited to: Iowa State University. Downloaded on May 16,2022 at 19:17:35 UTC from IEEE Xplore. Restrictions apply.

C. Device Fabrication and Packaging

UGFET and CMFET devices are fabricated through a commercial foundry (i.e. MOSIS AMIS 1.6 µm technology). The silicon chip comprises several devices of various dimensions and is bonded in a 40-pin DIP package (Fig. 6). All transistors are n-channel types. The UGFETs tested here has a gate width-to-length W/L ratio of 4.0µm /1µ6 m and total size of 14.4µm×28.4µm.

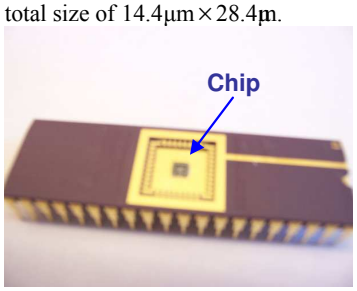

Fig. 6: Picture of the packaged chip with CMFET and UGFET devices.

III. Results

The performance of any sensor device is judged on its sensitivity, stability, and reproducibility. We tested the CMFET and UGFET devices (Fig. 1-2), and report their performance in this section. The measurements are repeated several times on devices with different sizes. We found a high degree of consistency among the data and the results are reproducible.

The basic drain current measurements are performed on CMFET (Fig. 7) and UGFET (Fig. 8) devices. The sensing area is left dry with no external charges. The drain current is a function of gate and drain voltages. Judging from the characteristics of the plots in Fig. 7 and 8, we can say that both the fabricated devices (CMFET and UGFET) work well as extended floating-gate field-effect transistors. The voltage given to the control-gate is able to induce a potential on the floating-gate and turn on the device [6]. The sensitivity of the floating-gate potential on the control-gate voltage follows from Eq. 1-3 and simulation results shown earlier.

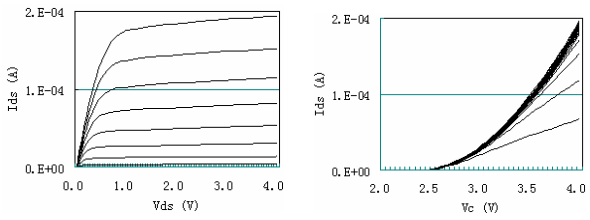

Fig. 7: Basic current-voltage measurements of a typical floating-gate CMFET biosensor with no charges over the sensing area. (Left) Drain current as a function of drain voltage at different control voltages. The control voltage increases from 2V (bottom curve) to 4V (top curve) in intervals of 0.2V. (Right) Drain current as a function of control voltage at different drain voltage. The drain voltage increases from 0V (bottom curve) to 4V (top curve) in intervals of 0.2V.

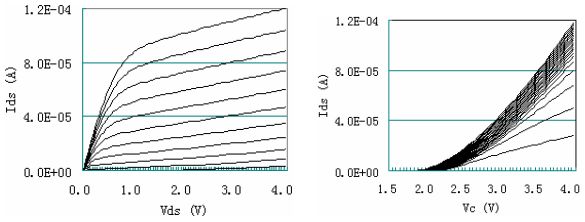

Fig. 8: Basic current-voltage measurements of our novel floating-gate UGFET biosensor with no charges over the sensing area. (Left) Drain current as a function of drain voltage at different control voltages. The control voltage increases from 2V (bottom curve) to 4V (top curve) in intervals of 0.2V. (Right) Drain current as a function of control voltage at different drain voltage. The drain voltage increases from 0V (bottom curve) to 4V (top curve) in intervals of 0.2V.

Next, the UGFET devices are tested with an electrolyte (potassium chloride, KCl) of different concentrations and a positively charged solution (poly-L-lysine). During the test, a ~1µL drop of a solution is carefully dropped over the sensing area. The devices have a spacer (i.e. passivation nitride layer) deposited. A LabView™ program is written for automated data-acquisition and controls the different electronic instruments (i.e. power supplies, function generator, multimeter, oscilloscope, and computer). For all the measurements, the control-gate voltage is slowly swept from 0V to 4V at a fixed drain voltage of 0.4V. The drain currents are then recorded. The current response to deionized (DI) water is used as reference for any threshold voltage shifts.

Poly-L-lysine is a positively charged amino acid solution and is commonly used as a substrate coating for cell adhesion. Its polycationic nature attracts the anionic groups of a biological sample and promotes adhesion. The UGFET devices respond to positive charges found in poly-L-lysine, as shown in Fig. 7. Since the surface charges Q_S on the sensing area are positive, threshold voltage will be reduced

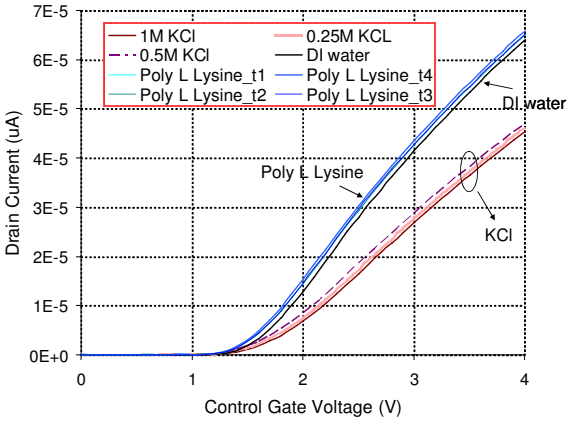

Fig. 9: Drain current as a function of the UGFET control-gate voltage for three different chemicals (Poly L Lysine, DI water and KCl salt) over sensing area. The curve from DI water is used as reference. The positively charged Poly L Lysine solution, dropped onto the sensing area and measured at four time intervals, shows a small overall shift to the left. The plots from KCl solutions show a large shift to the right.

Authorized licensed use limited to: Iowa State University. Downloaded on May 16,2022 at 19:17:35 UTC from IEEE Xplore. Restrictions apply.

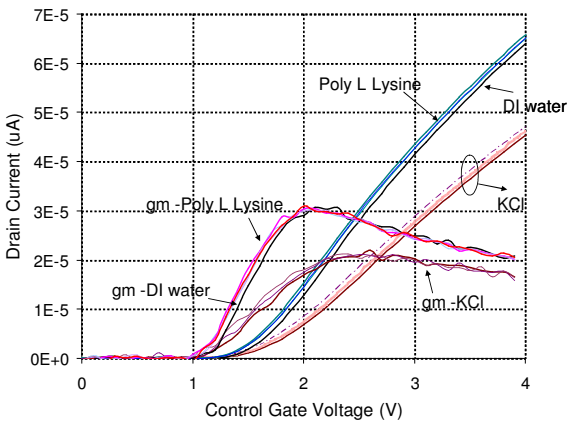

Fig. 10: Drain current and transconductance (gm) as a function of the UGFET control-gate voltage for three different chemicals (Poly L Lysine, DI water and KCl salt) over sensing area. The curve from DI water is used as reference. The threshold voltage shift is ~0.1V (negative shift) for Poly L Lysine and ~0.2V (positive shift) for KCl solutions.

due to a larger floating-gate voltage under the same control-gate voltage. The drain current curve is shifted left of the reference curve (due to DI water). Repeating the same measurements over time shows the drain current curves shift further to the left. Fortunately, this shift is marginal and might have been due to changes in the poly-L-lysine's concentration deposited onto the chip surface.

An electrolyte such as KCl is conductive solution due to the ions. During the tests, we ground the KCl solution with an external probe for stable measurements. Here, the capacitance between the floating-gate and the bulk C_{SF} plays a key role in modifying floating-gate potential. As shown in Fig. 9, grounded KCl solution shift the curve to right compare to DI water without ground, suggest that the net potential of DI water on top of the chip is not 0V, but higher than 0V.

The transconductance (gm) technique is an established method in semiconductor device physics for information about threshold voltage drifts. The transconductance (derivative of the drain current curves) plots are shown in Fig. 10. From the calculations, we see the threshold voltage is ~1.4V for poly-L-lysine solution, ~1.5V for DI water, and ~1.7V for grounded KCl solution. We notice the UGFET is capable of differentiating between positively charged poly-L-lysine and electrolyte solutions.

IV. Discussion

Future work is needed to find an appropriate spacer material that provides stable electrical and physical isolation to the UGFET's sensing area. In this direction, work is being done to test various polymer coatings of proper chemical compositions that allow us to reuse the chip multiple times. The interaction of microfluidic solutions with electronics platforms (especially floating-gate devices) still remains open to discussion [6].

We have demonstrated that the proposed UGFET devices can be fabricated with much smaller dimensions than present-day charge-modulated transistors. Reducing the sizes of the extended floating-gate transistors is important if they are to be considered potential candidates in VLSI circuit implementation. Thus far, this has not been feasible because of the large device area required. Fortunately, with suitable chemically-selective polymer coatings, UGFET VLSI microarrays could be constructed for various chemoreceptive and olfactory sensing applications.

V. Conclusion

This work presented a novel design for an extended floating-gate transistor (UGFET) that is scalable and fully compatible with the standard CMOS process. The fabricated devices perform well as charge-modulated sensors. The transconductance results show marked differences between positively-charged amino acids and electrolytes. Since most biological samples (single cells, proteins, DNA) have intrinsic charge, UGFET charge-modulated microarrays could serve as fast, portable, and inexpensive alternatives for biosensing applications.

Acknowledgment

The work is supported by the Electrical and Computer Engineering (ECpE) Department and the College of Engineering of Iowa State University.

References

[1] S.V. Dzyadevych, A.P. Soldatkin, A.V. El'skaya, C. Martelet, N. Renault, "Enzyme biosensors based on ion-selective field-effect transistors," *Analytica Chimica Acta,* vol. 568, pp. 248-258, 2006.

[2] G. Wrobel, R. Seifert, S. Ingebrandt, J. Enderlein, U. Kaupp, A. Offenhausser, "Cell-Transistor Coupling: Investigation of Potassium Currents Recorded with p- and n-Channel FETs," *Biophysical Jour.*, vol. 89, pp. 3628-3638, 2005.

[3] D. Kim, Y.Jeong, H. Park, J. Shin, P. Choi, G. Lim, "An FET-type charge sensor for highly sensitive detective of DNA sequence," *Biosensors and Bioelectronics*, vol. 20, pp. 69-74, 2004.

[4] P. Truman, P. Uhlmann, M. Stamm, "Monitoring liquid transport and chemical composition in lab on a chip systems using ion sensitive FET devices," *Lab Chip*, vol. 6, pp. 1220-1228, 2006.

[5] M. Barbaro, A. Bonfiglio, L. Raffo, "A Charge-Modulated FET for Detection of Biomolecular Processes: Conception, Modeling, and Simulation," *IEEE Trans. Electron Devices*, vol. 53, no. 1, pp. 158-166, 2006.

[6] N. Shen, Z. Liu, C. Lee, B. Minch, E. Kan, "Charge-Based Chemical Sensors: A Neuromorphic Approach with Chemoreceptive Neuron MOS Transistors," *IEEE Trans. Electron Devices*, vol. 50, no.10, pp. 2171-2178, 2003.

[7] M. J. Milgrew, P.A. Hammond, D.R.S. Cumming, "The development of scalable sensor arrays using standard CMOS technology," *Sensors and Actuators B*, vol. 103, pp. 37-42, 2004.

[8] F. Patolsky, B. Timko, G. Yu, Y. Fang, A. Greytak, G. Zheng, C. Lieber, "Detection, Stimulation, and Inhibition of Neuronal Signals with High-density Nanowire Transistor Arrays," *Science*, vol. 313, pp.1100-1104, 2006.

Authorized licensed use limited to: Iowa State University. Downloaded on May 16,2022 at 19:17:35 UTC from IEEE Xplore. Restrictions apply.